Critical assessment of pile modulus determination methods

Carlos Lam and Stephan A. Jefferis

Abstract: The elastic modulus of a concrete pile is an important parameter for the interpretation of load test results. This paper summarizes and assesses the methods available for its determination. Ten methods have been identified of which four are based on laboratory tests and the remainder on in situ pile instrumentation. Six of the methods have been used to interpret the modulus of a concrete pile subject to an axial load test. From the analyses, it was found that creep strains that developed during load-holding periods can have a significant effect on the modulus value if not allowed for when assessing the measured strain values. Based on a comparison of the derived pile loads the secant modulus method was found to be the most satisfactory. The tangent modulus method was also found to be a useful tool for investigating the effect of a partial steel casing — a feature of the method that has not been discussed before. Surprisingly, the theoretically correct transformed area equation had the worst performance, probably because of the chosen method for obtaining the concrete specimens on site.

Key words: concrete piles, instrumentation, pile load tests, strain gages, Young's modulus.

Résumé : Le module d'élasticité d'un pieu de béton est un paramètre important pour l'interprétation des résultats d'essais de chargement. Cet article résume et évalue les méthodes disponibles pour sa détermination. Dix méthodes ont été identifiées, dont quatre basées sur des essais en laboratoire, et les six autres basées sur l'instrumentation in situ du pieu. Six des méthodes ont été utilisées pour interpréter le module d'un pieu de béton soumis à un essai de chargement axial. À partir des analyses, il a été remarqué que les déformations de fluage développées durant les périodes de maintient des charges peuvent avoir un effet significatif sur la valeur du module, si ces déformations ne sont pas considérées lors de l'évaluation des valeurs mesurées de déformation. Selon la comparaison des charges dérivées sur les pieux, la méthode du module sécant s'est avérée être la plus satisfaisante. La méthode du module tangent est aussi apparue comme un outil efficace pour l'étude de l'effet d'une enveloppe partielle d'acier, caractéristique de la méthode qui n'a pas été discuté auparavant. Une observation surprenante est que l'équation pour l'aire transformée, correcte théoriquement, performe le moins bien, probablement en raison de la méthode choisie pour obtenir les échantillons de bétons sur le site.

Mots-clés : pieux de béton, instrumentation, essais de chargement sur des pieux, jauges à déformation, module de Young.

[Traduit par la Rédaction]

Introduction

Modern load tests on piles commonly include instrumentation to provide information on the load transfer mechanism so that the pile–soil interface properties can be back-calculated to verify design assumptions and optimize the final pile design. The instrumentation typically consists of strain gages and extensometers located at several critical locations along the pile for measurements of strain distribution and pile compression. Recent advances in the fiber-optic technology also allow continuous strain profiles to be acquired. Regardless of the method used, conversion of strain data into loads requires an assessment of the axial stiffness of the pile (EA) and the use of Hooke's law written in the following form:

$$[1] \qquad P_i = (EA)_i \varepsilon_i$$

where P_i is the load in the pile at any instrumentation level, i; E is the elastic (Young's) modulus of the composite pile material (concrete and any steel); A is the cross-sectional area of the pile; and ε_i is the measured strain at level i.

The conversion is relatively straightforward for steel piles, where for all practical purposes the elastic modulus can be taken as 205 ± 5 GPa, however, for concrete piles it is more complicated. First, concrete is a variable material; its properties can differ between batches even of the same mix design and may contain local defects, such as voids and microcracks. Second, as the modulus value of concrete is a function of both strain and strain rate (Lee et al. 2006; Stokes and Mullins 2009), tabulated values from design codes are not suitable for the purpose of load test interpretation. Third, for maintained load tests, where the load may be held for up to 24 h (ASTM 2007), the situation can be complicated further by the development of concrete creep strain, which can significantly affect the calculated value of the elastic modu-

Received 30 January 2011. Accepted 19 July 2011. Published at www.nrcresearchpress.com/cgj on 23 September 2011.

C. Lam. Department of Engineering Science, University of Oxford, Parks Road, Oxford, Oxfordshire, OX1 3PJ, UK.
S.A. Jefferis. Environmental Geotechnics Ltd., St Mary's Grove, 4 Adderbury Park, Adderbury, Banbury, Oxfordshire, OX17 3EN, UK; Department of Engineering Science, University of Oxford, Parks Road, Oxford, Oxfordshire, OX1 3PJ, UK.

Corresponding author: Carlos Lam (e-mail: carlos.lam@eng.ox.ac.uk; carloslam@hotmail.co.uk).

lus. Although in the past the need for the creep strain correction has only been emphasized for long-term load measurements over a period of perhaps several weeks or months (e.g., Dunnicliff 1993; Fleming et al. 2009; Ooi et al. 2010), as will be shown later creep is also an important consideration for tests that last only a few days.

To provide a practical procedure for the estimation of E, earlier investigators have proposed many different methods ranging from simple correlation with compressive concrete strength to full-scale instrumented dummy piles. Despite the importance of this parameter to the accuracy of the interpretation of pile test results, an overview of the available methods and their respective limitations has not been found in the literature. Guidance on this matter is also scarce in the current design manuals, standards, and specifications. For example, in the drilled shaft manual of the Federal Highway Administration, O'Neill and Reese (1999) touch upon the issue, mentioning one possible method for determining E. In Hong Kong, GEO (2006) suggests two methods for cast-in-place piles, whereas in the UK the guidance section of the ICE Specification for Piling and Embedded Retaining Walls is silent on the issue (ICE 2007). As a result, little consistency exists in the literature on the determination of E, and this no doubt affects the interpretation of the many pile load tests carried out each year around the world.

This paper first presents a general discussion of all the determination methods for E available in the public domain. To assess their respective performance and limitations, selected methods are then used to derive the E values and the interpreted loads of a bored pile (drilled shaft) tested by the maintained load method with holding periods after each load increment. The comparison also allows the effects of creep strain and partial steel encasement to be considered; both of these issues are commonly encountered in practice but seldom discussed. In this paper, discussions are limited to static load tests where the loading rate is slow enough that its effect on pile modulus is generally not a concern. Stokes and Mullins (2009) discuss the effect of strain rate as it pertains to the interpretation of rapid load test results.

Review of existing methods

After a detailed literature survey, the authors have identified 10 different methods that can be used to derive E for the interpretation of instrument data from static load tests. These methods are summarized in Table 1 together with a brief description of their key input parameters and references to the associated publications. The methods can be categorized into two broad groups: those that are suitable for piles having uniform cross-sectional geometry and composition along their lengths, and those for piles with significant change. Within each group, further classification can be made based on the specific methodology: laboratory test or in situ pile instrumentation. Note that apart from the tangent modulus method which is so-named by its proposer, all the other methods have no generally accepted names and are identified according to their principal characteristics.

The following review starts with a discussion of the condition of geometrical (strain) compatibility, which is a fundamental assumption for the determination of pile modulus. Discussions of each individual estimation method then follow.

Geometrical compatibility and the transformed area equation

Reinforced concrete is a composite material. To estimate the stress level in a concrete pile, it is necessary to assume that the measured strains from the strain gages are representative of the entire cross section and not just the individual component to which the gages are attached. In other words, ε_g equals ε_c and ε_s, where the subscripts "g", "c", and "s" represent gage, concrete, and steel, respectively. This assumption is called the condition of geometrical compatibility. An early debate about the validity of this assumption in relation to pile load testing can be found in the discussion section of Grime (1934). Dunnicliff (1993) states that well-designed "sister bar" strain gages (also known as rebar strainmeters) have small inclusion effects and the measured strain will be equal to that in the concrete and in the steel reinforcement. To test the assumption of strain compatibility, Holman (2009*a*) conducted a load test on a micropile with spot-weldable strain gages attached to the reinforcing steel and embedment gages in the cement grout that was used to form the pile. A difference of between 14% and 43% between the two readings was found, but neither of them consistently showed higher or lower strains than the other. Taking into account the possible effect of shear stress transfer at the grout–steel interface, it was concluded that the difference was minor. Similar evidence of geometrical (strain) compatibility in reinforced concrete piles was also given by Gregersen et al. (1973). Based on these findings, this assumption appears to be reasonable as long as well-designed strain gages are used. Information on strain gage design can be found in Dunnicliff (1993).

In addition to the actual strain measurement, the assumption of geometrical compatibility is also essential for the interpretation of test results. In the case of a reinforced concrete pile, taking force equilibrium between the concrete and the reinforcing steel in a pile section and assuming strain compatibility (i.e., ε_c equals ε_s) one can write the following equation:

$$[2] \qquad EA = E_c A_c + E_s A_s$$

Equation [2] states that the overall axial pile stiffness is simply the sum of the concrete and steel stiffnesses. It can be extended to include the contribution of other elements, such as a permanent steel casing at the pile perimeter, provided that there is no slippage at the interface and strains remain compatible. This particular issue will be discussed in greater detail later.

Methods based on laboratory tests

A number of methods were identified that use laboratory test data and these are discussed in the following sections.

Transformed area method

With the moduli and cross-sectional areas of both steel and concrete known, eq. [2] can be used to estimate the composite pile modulus (E). This approach is referred to as the transformed area method. When using this method, the respective areas of steel and concrete can be estimated from

Table 1. Summary of determination methods for pile modulus.

Pile geometry and composition with depth	Basis of method	Method	Equation	Key required parameter(s)	References
Uniform	Laboratory test	Transformed area[a]	$E = (E_cA_c+E_sA_s)/A$	E_c from laboratory tests on concrete cubes or cylinders for compressive strength or elastic modulus. Samples prepared during casting or cored from completed pile.	O'Neill and Reese (1999); Hayes and Simmonds (2002); GEO (2006)
		Uncorrected area	$E = E_c$		Ooi et al. (2010)
		Dummy pile	$E = P/A\varepsilon$	ε of the instrumented dummy pile.	Lacy (1979); Fleming (1992)
	Pile instrumentation	Implicit	$P_i = P_1\varepsilon_i/\varepsilon_1$ where $P_1 \approx P_h$	ε at the uppermost strain gage.	Sellers (2003)
		Linearly elastic	$E = \Delta P/A\Delta\varepsilon$	$\Delta\varepsilon$ at the uppermost strain gage or extensometer.	O'Riordan (1982); Omer et al. (2002)
		Tangent modulus	$\sigma = a\varepsilon^2 + b\varepsilon$ $E_t = d\sigma/d\varepsilon = a\varepsilon + b$ $E = 0.5a\varepsilon + b$	$d\sigma/d\varepsilon$ from one or several sets of strain gage–extensometer data. a and b from E_t–ε plot.	Fellenius (1989, 2001)
		Secant modulus	$E = P/A\varepsilon$	ε at the uppermost strain gage.	Shi (1996); Deschamps and Richards (2005); GEO (2006)
			$E = PL/A\delta$	δ at the uppermost extensometer.	England and Fleming (1994); Shi (1996); Hanifah and Lee (2006); Ali et al. (2008)
Nonuniform	Laboratory test	Dummy pile	Elastic solutions	ε in longitudinal, radial, and circumferential directions.	Omer et al. (1995, 2002)
	Pile instrumentation	Tangent modulus and transformed area	$E_t = d\sigma/d\varepsilon = a\varepsilon + b$ $E = 0.5a\varepsilon + b$ $E = (E_cA_c + E_sA_s)/A$	$d\sigma/d\varepsilon$ from one or several sets of strain gage data. a and b from E_t–ε plot. E_c and E_s for each pile section.	Holman (2009*b*)
		Secant modulus and transformed area	$E_c = (P - E_sA_s\varepsilon)/\varepsilon A_c$ $E = (E_cA_c + E_sA_s)/A$	ε from uppermost strain gage. E_c and E_s for each pile section.	Omer et al. (2002); Brown et al. (2006); Lee et al. (2006)

[a]The transformed area method can also be used to estimate the modulus of piles with nonuniform cross-sectional areas and (or) compositions.

the construction records (e.g., concreting or borehole calliper records) and the steel modulus can be taken as 205 ± 5 GPa. Because the errors involved in using design code values of concrete modulus (E_c) are considered too great for the purpose of load test interpretation, E_c is commonly determined on laboratory specimens that are either prepared during casting or obtained by coring the completed piles. Two further options are then available in terms of testing: measure E_c directly on the specimen or derive it from the unconfined compressive cylinder strength (f_{cyl}) via correlation equations. These equations typically take the form $E_c = k(f_{cyl})^{0.5}$ (ACI 2008) or $E_c = k(f_{cyl})^{0.3}$ (Eurocode 2, CEN 2004) where k is a constant of proportionality depending on the density of the concrete and the design code. As a result, the derived value of E_c is heavily influenced by the choice of sampling location, testing method, and the local governing standard. Despite the possible inaccuracies, this method is one of the few methods that are commonly mentioned in design manuals, such as O'Neill and Reese (1999) and GEO (2006).

Uncorrected area method

The uncorrected area method is a simplified version of the transformed area method, where the stiffness contribution of the reinforcing steel is ignored and eq. [2] becomes $E = E_c$. Although this method has been used in situations where a benchmark value is needed, it should be recognized that the errors can be large and its use should be avoided. Shi (1996) expresses a similar view.

Dummy pile method

To reduce the uncertainty arising from different sampling and testing strategies, short instrumented dummy piles were used by Lacy (1979) and Omer et al. (2002) for the direct determination of the composite pile modulus. In these studies, the dummy piles were between 2 and 3 m long and were load tested in a laboratory. The treatment of the test data in the two papers was, however, rather different — Lacy (1979) produced a pile modulus curve over a range of stress levels (secant modulus method) and Omer et al. (2002) back-calculated the elastic moduli and Poisson's ratios for each of the individual structural elements (elastic solution); these methods will be discussed in more detail later. Fleming (1992) also discussed the possibility of casting a dummy pile on site, which then could be extracted and tested in a load frame concurrent with pile loading. Fleming's approach allows the dummy pile to be cured under similar moisture conditions to the test pile — a feature recognized by Dunnicliff (1993) as important.

Methods based on pile instrumentation – uniform pile geometry and (or) composition

A common alternative to the laboratory-based methods is to measure the pile modulus in situ. This is usually done by placing a set of strain gages near the pile head so that the loads at this level can be taken as the applied loads. E is back-calculated from the known stresses and the measured strains. The resulting E, which can take a single value or be in the form of an equation depending on the chosen method, is then applied to the data from gages at other levels for strain-to-load conversions. Although the concept is simple, the stress–strain (σ–ε) curve used for calibration has been interpreted in different ways by previous researchers. Four methods have been found, namely the implicit method, the linearly elastic method, the secant modulus method, and the tangent modulus method.

Implicit method

Sellers (2003) reported a method that obviates the need for a known value of E but still allows the calculation of pile load at any depth; hence referred to as the implicit method. Sellers (2003) proposed that the pile load at any instrument level, i, can be obtained by reducing the applied load P_1 by the ratio of the strain at that depth to the strain recorded at the uppermost set of gages, that is, $P_i = P_1(\varepsilon_i/\varepsilon_1)$ where P_1 and ε_1 are the load and strain at the first instrument level, respectively, and P_1 is taken as the applied head load (P_h). The underlying assumption is that, under any given head loads, the axial pile stiffness, EA, is the same throughout the pile. Therefore, its value does not need to be known as it cancels out of the equation. For piles with constant modulus, but nonuniform cross-sectional areas, the equation can be modified to retain the area ratio thus becoming $P_i = P_1(A_i\varepsilon_i/A_1\varepsilon_1)$. The elastic modulus of concrete is strongly dependent on the stress or strain levels. It follows that the assumption of uniform stiffness necessary for this method, whilst reasonable for end-bearing piles where the stress level changes little along the pile, may introduce significant errors for friction piles where the stress level near the base will be very different from that at the top because of shaft resistance.

Linearly elastic method

As its name suggests, this method assumes a linear σ–ε relationship for the pile material so that E can be taken as the slope of the curve, $\Delta P/A\Delta\varepsilon$. Because this method only uses the slope of the σ–ε curve, any residual strains at zero load are discounted and this is probably why the two identified studies, which used this method, both included many load cycles in the tests (O'Riordan 1982; Omer et al. 2002). Unlike the implicit method, which allows E to be varied under different head loads, E obtained from this method is not a function of strain or stress levels. Although at first sight this method may appear to be suitable for tests with many load cycles because of its ability to capture the degradation of E, one needs to bear in mind that the stress ranges, and therefore the amount of modulus degradation (if any) at the uppermost gage level, can be very different from those further down the pile even for the same loading cycle.

Secant modulus method

Unlike the two previous methods, the secant modulus method truly takes into account the strain dependence of the pile modulus, and hence allows E to increase down the length of the pile because of the reducing stress and strain levels. To use this method, one first needs to compute a modulus curve, E, from each pair of measured stress and strain values obtained in the test, as recorded by the uppermost gage level. The modulus value determined in this way is commonly referred to as the secant modulus and hence the name of the method. The resulting modulus values are then plotted against ε and their relationship modeled with a best-fit curve or line. The fit establishes an equation for the secant modulus as a function of the measured strain, which is then

applied to the other gage levels in the pile to convert the measured strains into loads. This method assumes that the E–ε relation developed for the gage level near the pile head can be applied to the remainder of the pile. In most cases, such an assumption can be validated, at least for the top part of the pile, by the tangent modulus method, which is discussed below.

For the strain measurements, sister bar strain gages or extensometers have both been proposed by practitioners (England and Fleming 1994; Shi 1996; Hanifah and Lee 2006; Ali et al. 2008). The main difference between the methods of these practitioners is the length over which the strain is measured. For sister bar strain gages, the effective gage length is only about 50 mm. For retrievable-type extensometers, the gage length is the distance between the first anchor point at the pile head and the second one at about half a metre to several metres below the pile head.

Tangent modulus method

Fellenius (1989, 2001) proposed a method called the tangent modulus method, and it has become very popular among both practicing engineers and academic researchers. The main advantage of this method is that it considers the modulus of the pile materials not only at the pile head but at all instrument levels. For gage levels down in the soil, this method takes advantage of the fact that, after full mobilization of shaft resistance, the σ–ε response of the pile material is effectively that of a free-standing column provided that the soil can sustain its peak strength (i.e., show elastic – perfectly plastic type behavior). The σ–ε curve is assumed to follow a second-order polynomial, so that the tangent modulus, E_t, has a linear relationship with strain. The secant modulus, E, which is still the modulus required for strain-to-load conversion, is then calculated from the slope and intercept of the E_t line. When applied to the gage level near the pile head where the pile is unaffected by the shaft resistance, the tangent modulus and the secant modulus methods theoretically give the same results. As the tangent modulus method involves differentiation of load and strain values, errors in these numbers will have a larger effect on the modulus evaluation than for the secant modulus method.

The equations for the tangent modulus method are shown in Table 1. As full mobilization of the shaft resistance is required for this method to work at its best, the pile diameter has to be small and (or) the applied load large. For example, the pile used by Fellenius (2001) for illustration of the method had a diameter of only 357 mm. In a subsequent discussion of the method, Fellenius (2009) added that the strain in the pile should ideally exceed 500 με and the test load should mobilize at least half of the strength of the pile material. Hayes and Simmonds (2002) also noted that for bored piles the measured strains at the planes of interest (i.e., the strain gage levels) should preferably be more than 200 με.

Methods based on pile instrumentation — nonuniform pile geometry and (or) composition

Combined secant modulus, tangent modulus, and transformed area method

As discussed earlier, when in situ instrumentation is used a pile modulus value determined from a load–strain curve near the pile head is applied throughout the pile. Although this approach works well for piles with uniform or near-uniform cross sections, piles with significant changes in either their geometry or structural composition require fuller analysis. Nonuniform cross sections may occur if a long casing is used in the upper portion of a pile or if there is a design requirement for an enlarged base or a grouted base section. To account for the changes in pile stiffness, a common approach is to separate the contribution of each of the individual structural elements from the composite modulus estimated for the pile head, and then recombine them for other depths with different cross-sectional properties. To do this, most engineers have chosen to combine the transformed area equation with either the secant modulus method (Omer et al. 2002; Brown et al. 2006; Lee et al. 2006) or the tangent modulus method (Holman 2009*b*). In an alternative approach for piles with only short casings, Liew et al. (2004) disregarded the data from the uppermost strain gages, which were located within the casing, and used the gage results at the next level for modulus calibration. This approach avoids the labour of separating and recombining the moduli of each element, but as the gages used for calibration are now deeper into ground, the pile load acting at the gage level may no longer be equal to the head load. This can affect the accuracy of the interpretation.

Dummy pile method

To quantify the influence of the steel casing, Omer et al. (2002) carried out laboratory tests on a heavily instrumented dummy pile both with and without the casing. From the test results, the elastic moduli and Poisson's ratios of the concrete core, reinforced concrete, and the steel sections were back-calculated using an elastic solution developed by Omer et al. (1995). Although this may be a way of analyzing the problem, it does not account for the strain dependency of the modulus and the potential for differences between the properties of concrete prepared and cured in the laboratory versus on site. However, if these issues are not a concern, then this method does offer the advantage of accounting for the local stiffening effect of reinforcing steel bars on concrete (i.e., the variation of E across a pile's cross section).

Test pile details

Geometry and instrumentation details

To assess the impact of the choice of method on the derived value of E and the pile load distribution, selected methods have been used to interpret the test results of a bored cast in situ concrete pile (drilled shaft) subject to a "slow" maintained load test. The test pile had an embedded length of 27.0 m and a stick-up length of 0.5 m. The nominal diameter was 1.20 m, although the actual diameter of the upper 8.0 m length was 1.26 m as a temporary casing, removed during concreting, was used during construction. The total cross-sectional area including the steel casing was therefore 1.2469 m^2. The pile was reinforced axially with twelve 32 mm ribbed (deformed) steel bars (total area of steel 0.0097 m^2) in the upper half of the pile and four bars (total area of steel 0.0032 m^2) in the bottom half. To create a pile head suitable for the load test, the upper 1.2 m of the pile was encased in a steel casing (total area of steel 0.0587 m^2). The

concrete used was a self-compacting concrete with a target slump of 185 mm and design characteristic (5%) cube and cylinder strengths of 35 and 28 MPa, respectively. According to Eurocode 2, the expected mean cylinder strength was 36 MPa for this concrete strength class.

The pile was instrumented with sister bar strain gages (model VWS-4000 from MGS Geosense, Suffolk, UK) at five different levels: 0.75, 6.2, 14.9, 19.4, and 26.5 m from the pile head. At each level, a set of four gages was installed to account for the effect of load eccentricity due to construction imperfections and also to provide some degree of instrument redundancy. Retrievable extensometers (model A-9 from Geokon Inc., New Hampshire) were also installed throughout the pile to measure pile compression. Figure 1 shows the details of the pile. Figure 2 shows a photograph of the sister bar strain gages and the steel pipes (total area of steel 0.0079 mm^2) in which the retrievable extensometers were installed during the test. The steel pipes also doubled up as the access tubes for cross-hole sonic logging. No dummy piles were cast either on site or in laboratory.

Ground conditions

The test pile is located in the Stratford area of east London, UK. The ground conditions are typical of those in that area, consisting of a layer of made ground followed by the Lambeth Group and Thanet Sand. However, because of the construction of a nearby tunneling project, the thickness of the made ground was increased by deposition of the excavated materials to about 7 m, and the groundwater table in the Thanet Sand was permanently lowered to about 3 m below the toe level of the test pile. Standard penetration tests (SPTs) were carried out at a number of boreholes near the test pile to help establish the soil parameters. Figure 1 shows the idealized soil, pore-water pressure, and SPT N-index profiles. Table 2 also shows the soil parameters used for the preliminary design. As there were only a few effective stress tests included in the laboratory test program, some of the effective stress parameters (c' and ϕ') and the earth pressure coefficients (K_0) in Table 2 were estimated by reference to the relevant literature (e.g., Georgiadis et al. 2003; Hight et al. 2004).

Laboratory concrete test results

During the construction of the pile, specimens of fresh concrete were taken from the delivery trucks for the determination of the compressive cube strength (f_{cube}) and elastic modulus (E_c) on the day the pile was tested. From the results, the average f_{cube} was 50.4 MPa and the average E_c was 29.3 GPa. If the equivalent cylinder strength (f_{cyl}) is taken as 75% of the cube strength, it will have a value of 37.8 MPa, which ties in with the expected value of 36 MPa. Substituting this computed f_{cyl} into the design code equations therefore gives correlated E_c values of 28.9 GPa (ACI) and 32.8 GPa (Eurocode 2), which correspond reasonably well with the average value measured on the concrete specimens of 29.3 GPa. The latter measured E_c value will be used to estimate E in the following comparison as it is the more direct.

Load test method

The pile load test was carried out 28 days after construction by the maintained load method, which is the standard

Fig. 1. Test pile details and ground conditions.

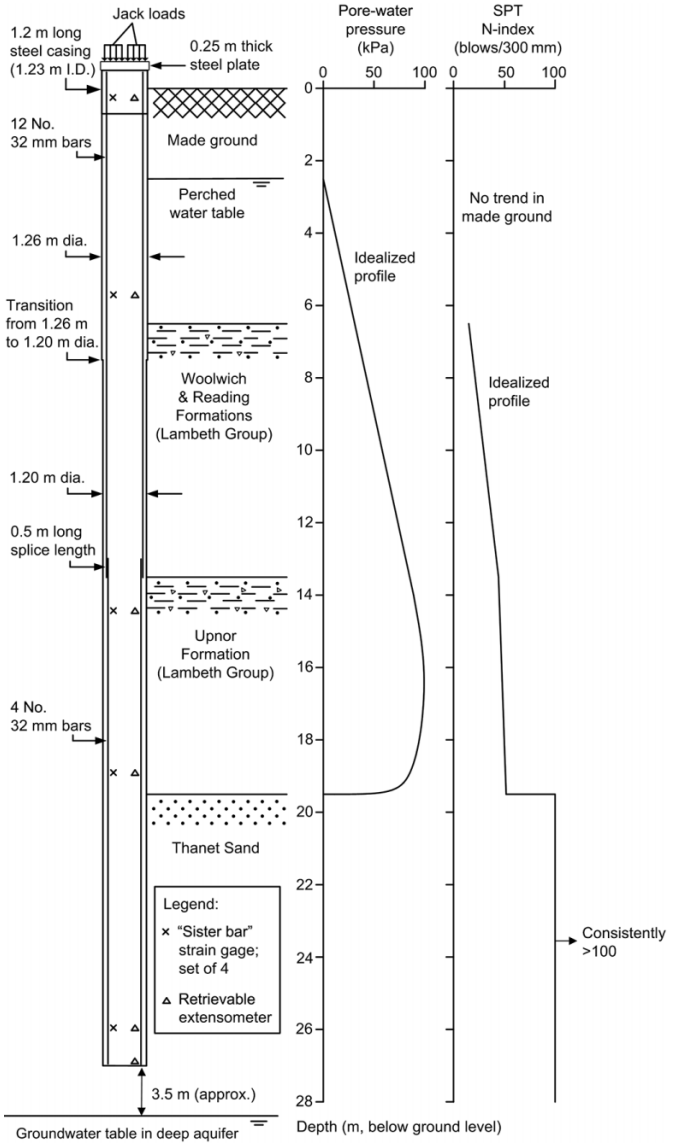

method in the UK. Load-holding periods after each load increment and an unload-reload loop were included in the test in accordance with the local governing specification for load testing — SPERW (ICE 2007). The loading sequences actually differed slightly from the specification to incorporate a higher proof load, that is, 100% design verification load (DVL) plus 100% specified working load (SWL) following the terminology of SPERW. Figure 3 presents the load–movement records of the test, showing the applied head load versus the head and toe movements. The difference between these two curves is the total shortening of the pile as measured by the extensometers. It can be seen that there is creep movement of the pile at each of the load-holding stages. At the pile head, this movement was caused by a combination of creep in the concrete and also movement in the soil, whereas at the pile toe the settlement was only the result of the movement of the soil. Time-dependent soil movements adjacent to the pile shaft will potentially transfer loads to greater depths in the pile, thus increasing the overall axial creep of the concrete.

Fig. 2. Sister bar strain gage and steel tube for installation of retrievable extensometer.

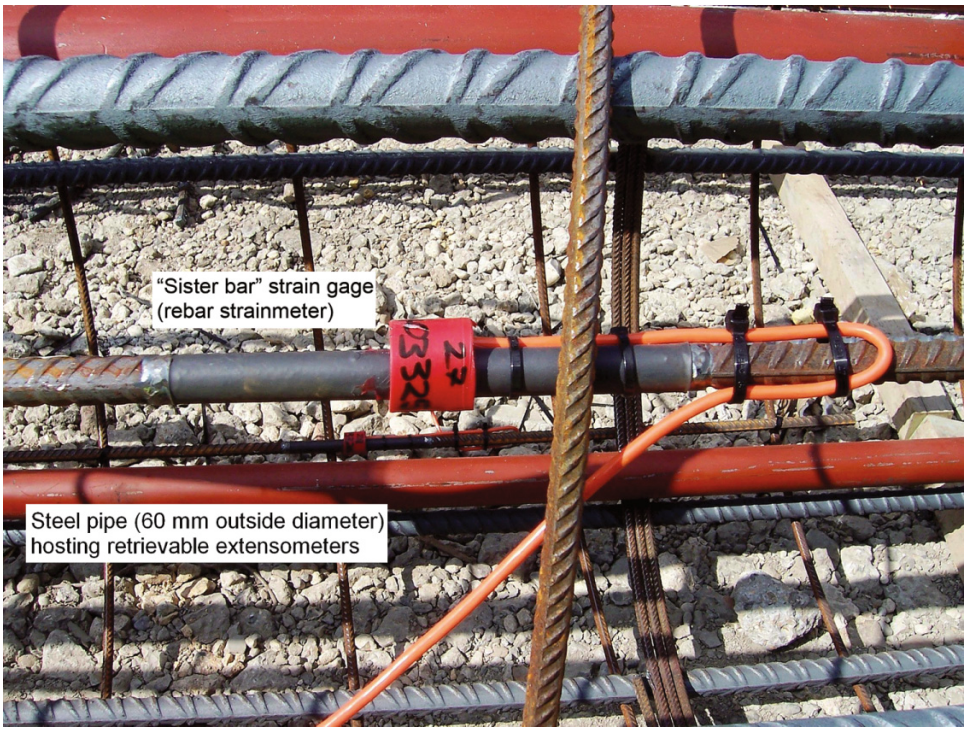

Table 2. Summary of soil parameters for preliminary pile design.

Soil	Saturated unit weight, γ_{sat} (kN/m^3)	Undrained shear strength, S_u (kPa)	Adhesion factor, α	Effective cohesion, c' (kPa)	Angle of shearing resistance, ϕ' (°)	Coefficient of earth pressure at-rest, K_0
Made ground	18	—	—	0	30	0.5
Woolwich and Reading Formations (Lambeth Group)[a]	20	67.5 + 18.64Z	0.6	0	26	1.15
Upnor Formation (Lambeth Group)	21	198.0 + 6.34Z	0.6	0	33	1.15
Thanet sand	19	—	—	0	36	1.15

[a]At the test site, the Woolwich Formation consists of laminated beds and Lower Shelly clay, and the Reading Formation includes Lower Mottled clay.

Fig. 3. Load–movement curves.

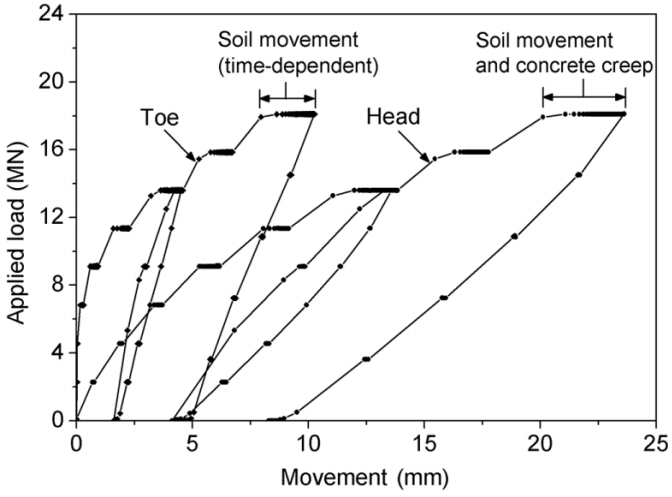

During the test, the actual loading and unloading rate, excluding the load-holding periods, was 0.45 MN/min which corresponds to 0.006 MPa/s for a diameter of 1.26 m. This means that each load increment of 2.28 MN (25% DVL or SWL) took 5 min to complete. It is interesting to note that this loading rate is significantly lower than the 0.6 ± 0.4 and 0.24 MPa/s specified by the BSI (1983) and ASTM (2002), respectively. With a loading rate this low, it is reasonable to assume a negligible strain-rate effect on the pile concrete. However, as will be shown later, the relatively high loading rates used by the standard laboratory test methods could become a potential source of error in the determination of E by some methods.

End effect on strain values

As the uppermost set of strain gages was placed close to the pile head to minimize the loss of the pile load due to shaft resistance, it is worth considering the end effect and its potential impact on the strain gage results. Saint-Venant's principle (named after the French scientist A.J.C.B. de Saint-Venant) states that any localized stresses will dissipate and

the stress distribution will become practically uniform at a distance sufficiently far from the location of the load. For axially loaded members, Timoshenko and Goodier (1970) show that this distance is approximately equal to the width of the member, although some also believe that this distance should be longer (Dunnicliff 1993). This rule of thumb of one member width (or height) has also been adopted by structural design codes, such as ACI (2008), for a wide range of loading cases and recommended by practitioners, such as Hayes and Simmonds (2002), for pile testing using O-cells.

In the subject test pile, the uppermost set of strain gages was placed at a distance less than one pile diameter from the pile head, and this was because the design engineer was unaware of this rule. Despite this flaw in the load test design, the thick steel plate below the two hydraulic cylinders should reduce this undesirable effect by transmitting the jack load uniformly onto the pile head (Fig. 1). The use of four strain gages at each instrumentation level should also capture some of the nonuniform strain distribution in the pile — this method is recommended by Dunnicliff (1993) after recognizing the practical difficulty of having a long stick-up length above the ground surface for bored piles. Furthermore, as will be shown later by the tangent modulus method, the measured response of E at the uppermost two sets of strain gages are effectively the same, thus suggesting a negligible end effect on the overall strain values in this pile.

Installation effect on strain values

Fellenius et al. (2009) reported a case study of long-term monitoring of strain in some grouted cylindrical concrete piles. It was found that the strain readings were influenced, among other things, by the heating from the hydration of the cement and the subsequent cooling, despite the fact that the sister bar strain gages had been found to be not particularly sensitive to temperature changes. This finding was attributed to the internal strain distribution caused by the different thermal-expansion coefficients of the steel and the concrete. To examine whether the strain gages used for the subject test pile were also affected during their installation, the strain values were recorded at three critical stages: in the construction yard, immediately after concreting (in practice this meant about 3 h after pouring), and just before commencement of the load test.

Figure 4 presents the change in the strain values referenced to the baseline values taken in the yard. It can be seen that the gage readings were indeed affected by the installation process, causing them to drop immediately after concreting and then to increase slightly during curing. This indicates that the gages first experienced a compressive force, probably as a result of the internal strain distribution due to the hydration heat. As the concrete cooled, this process reversed resulting in a partial recovery of some of the compressive strains and even some tensile strains near the bottom of the pile. This overall pattern of change in the strain values is rather similar to those presented by Fellenius et al. (2009) although the actual values are, of course, different. As it is not possible to separate these installation effects from the strains caused by the residual load that may have built up during the same period, the effect of residual load is considered later by a different method.

Fig. 4. Effect of installation on strain gage readings.

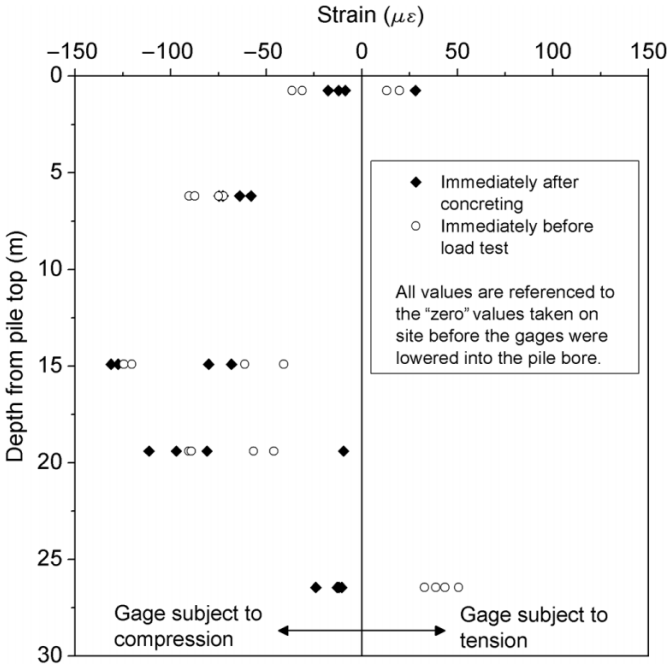

Deformation behavior of pile material

Stress–strain response of pile materials

Figure 5*a* shows the compressive σ–ε curve for the pile materials as recorded by the strain gages at the five instrumentation levels. The plotted strain values are the average gage readings at each level. To separate the strains caused by the installation process from those caused by the applied load, these strain values are all referenced to their values recorded at the start of the load test. As can be seen, the measured strain values increased significantly during the load-holding periods and can be seen as both time and stress dependent. To highlight the effect of creep strains on the measured values, Fig. 5*b* shows again the readings of the uppermost set of strain gages (0.75 m below pile head), but now two curves are given in the figure: the dotted line plots the actual measured response, and the solid line plots the immediate response, indicating a "correction" for the effect of concrete creep strains. For the purpose of correction, creep strains are defined here as the strains that develop during the load-holding periods. As the application of each load increment took about 5 min, the potential error caused by this assumption, using the creep prediction method given in CEN (2004), is about 3.5% of the total value.

As can be seen in Fig. 5, the two curves show that a significant amount of concrete creep (ε_{cc}) developed during the load-holding periods, resulting in a total of about 200 με at the end of all the loading stages. If these creep strains are removed, the σ–ε curve then plots as a hysteresis loop with negligible residual plastic strains. This means that the true σ–ε response was nonlinearly elastic and the corrected strains can now be described as elastic strains. However, despite the correction, a small amount of plastic strain (6 με), caused by the unload–reload loop, is still present and may just be noticed on the corrected curve at 11.4 MPa. Although these plastic strains are relatively small (<1% of total) and hence

Fig. 5. Stress–strain curves of pile material from sister bar strain gages: (*a*) measured response at all instrumentation levels; (*b*) measured and corrected response at the uppermost level.

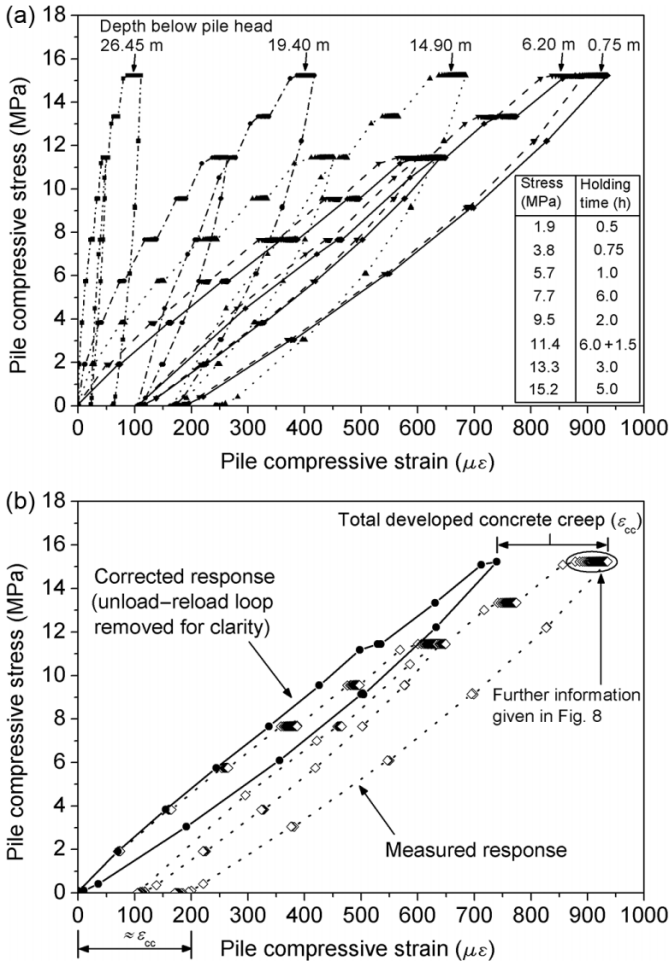

negligible in this case, they could become significant in tests that include many unload–reload loops (see e.g., O'Riordan 1982; Omer et al. 2002). They could become another major source of error in the strain-to-load conversion process if not allowed for. With this in mind, the so-called quick test method (e.g., procedure A of ASTM 2007) seems to be a much better approach, as it does not require any significant load-holding periods nor unload–reload loops. Such a test method results in a "cleaner" stress–strain curve that is free of these extraneous influences.

The aforementioned creep correction procedure was also applied to the other strain gage data given in Fig. 5*a*, and Fig. 6 shows the corrected strain profiles along the depth of the pile for the different loading stages. For comparison, the uncorrected strain profile at proof load (18.1 MN) was also given on the plot. It can be seen that the amount of the "creep portion" gradually decreases with depth, which is expected due to the reducing stress level in the pile as shown by the strain profile itself.

To compare the results of the different strain measurement techniques, Fig. 7 shows the output of the uppermost retrievable extensometer both in millimetres and in converted microstrains. Unlike the measured response of the strain gages (dotted line and white diamonds in Fig. 5*b*), the extensometer

Fig. 6. Strain profiles at different loading stages.

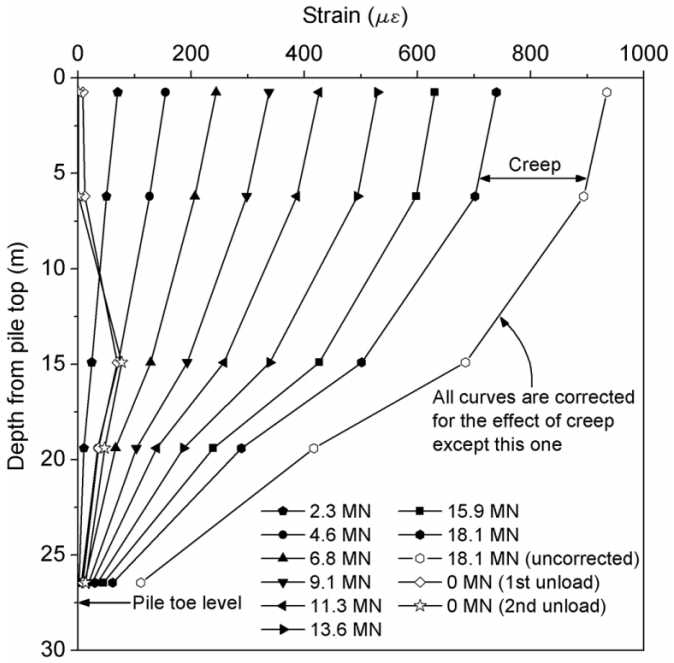

Fig. 7. Stress–strain curve of pile material from the uppermost extensometer.

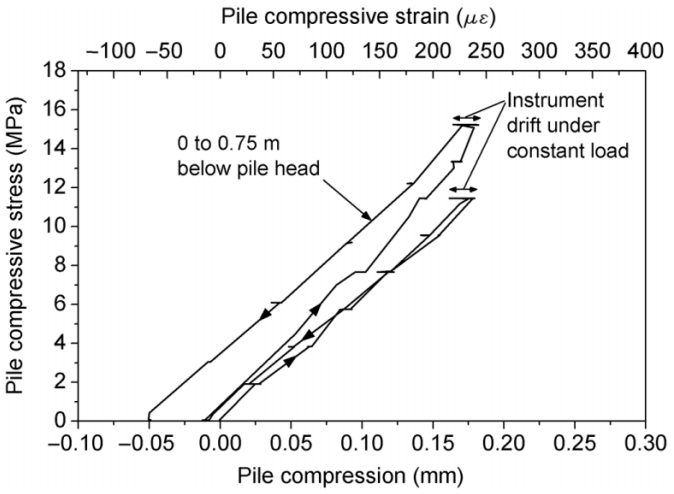

did not detect any creep during the load-holding stages, but instead displayed a noticeable amount of instrument drift. At proof load, the amount of drift was about 0.02 mm, which is equivalent to 27 με over the gage length. Another problem with the extensometer was that the readings became negative on unloading, a problem that became more pronounced as the maximum stress level increased. The reasons for the apparent malfunction of the extensometer are not known, but it may have been due to debonding and slippage at one of the interfaces between the extensometer anchors, steel tube, and the pile concrete. Debonding at the steel–concrete interface is possible because of the smooth painted surface of the steel tube and the large difference in their modulus values leading to high shear stress to be carried at the wall (Fig. 2). For this reason, the extensometer records were not used in the further analysis of the test data.

Creep development behavior

As most of the modulus determination methods will make use of the corrected (total minus creep) strain values as given in Figs. 5*b* and 6, it is useful to check the so-defined creep values against those determined by the standardized methods just to ensure that they are reasonable. Such an assessment would also highlight the effects of nonuniform stress distribution (due to end effects and construction imperfections) and steel (due to the reinforcing bars, sonic logging tubes, and the external casing) on the creep behavior of the pile, as follows.

Figure 8*a* shows the creep strains of the four individual strain gages at the uppermost instrumentation level under proof load. It can be seen that, although they all start with a different strain value (given to the right of the curves), this value does not correlate strongly with the measured creep strain. For example, gage 1 had the second lowest starting strain but recorded the second highest creep strain. This suggests that the measured creep strains were not particularly sensitive to the nonuniform stress distribution across the cross section of the pile. The curves given in this figure also justify the decision to use four gages instead of two at each instrumentation level, as the result would be 10% higher or lower if only two were used.

Figure 8*b* shows the creep strain predictions using the laboratory-determined concrete parameters and the calculation method given in Eurocode 2 (CEN 2004). As Eurocode only covers the creep strain of plain concrete, the age-adjusted effective modulus method given in Wight and MacGregor (2009) was used to take account of the restraining effects of the various steel components in the pile. The result is interesting; the various steel components had a strong effect not just on elastic but also on the creep behavior of the pile. For example, including the reinforcing bars alone would reduce the prediction at 5 h from 77 to 61 με. If the effects of the logging tube and the external casing are also considered, then the predicted value would drop down to 33 με. If these predictions are correct, they will offer an opportunity to assess the contribution of the various steel components (i.e., the level of geometrical compatibility with the concrete). However, because all the current predictions underestimate the measured values, it is likely that the actual quality of the pile concrete was lower than that of the cubes tested in the laboratory. This is possible as, during casting, a certain volume of the excavation-support fluid (synthetic polymer in this case) may have intermixed with the fresh concrete and hence raised its water–cement ratio. To match the prediction of the scenario where only concrete and reinforcing bars contribute (the dotted line in the plot), the values of the two concrete parameters, E_c and f_{cyl}, would need to be reduced by 20%. As will be shown later, this degree of reduction is not unreasonable. An attempt was also made to match the case where all the steel components contribute (the solid line in the plot) but it turned out not to be possible. The highest creep value achievable for this case is 63 με (still 17 με short of the measured value) even when the parameter values are reduced by 80%. Any further reduction would lower the amount of the predicted creep. This is because, as the contribution of the concrete reduces, the steel would start to dominate the overall deformation behavior and, because steel does not creep, the predicted creep strain would reduce. Based on the finding of this "matching" exercise, it would appear that the pile concrete was weaker than expected and the external steel casing did not contribute to the deformation behavior of the pile. The last point will be reconsidered in the discussion on the tangent modulus method.

Fig. 8. Creep development of pile material: (*a*) individual strain gage results; (*b*) comparison with predicted values.

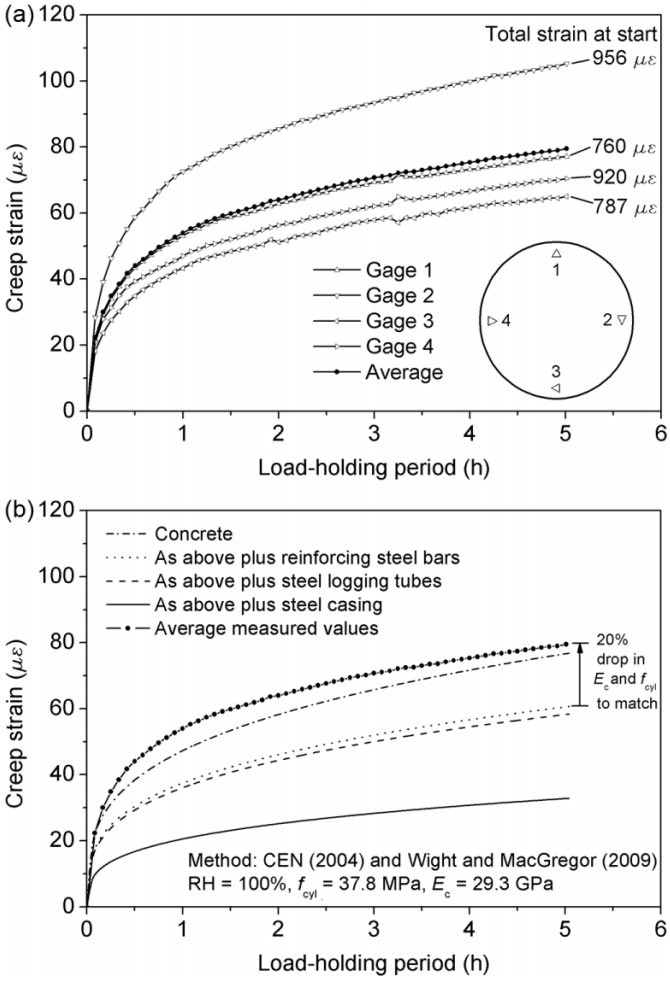

Pile modulus and interpreted load

Method selection

As shown in Table 1, the choice of an estimation method depends on two main factors: the availability of data (laboratory test result, pile instrumentation, dummy pile), and the uniformity or otherwise of the pile. Although no dummy piles were cast in this trial, the availability of the laboratory results and pile instrumentation data allowed the assessment of six methods, namely linearly elastic, tangent modulus, secant modulus, uncorrected area, transformed area, and the implicit methods. As the pile had no significant change in its dimension or composition with depth (Fig. 1), it was assumed to be uniform for the application of the tangent and the secant modulus methods. The assumption of uniform pile geometry and composition will be revisited when the effect of the steel casing is considered in the following section.

Derived modulus values and the effects of partial steel encasement and creep strains

The pile modulus (E) for linear response was first calculated by the linearly elastic method using the corrected σ–ε curves given in Fig. 5*b*. The E value over this stress (or strain) range was estimated to be 20.6 GPa.

Following the previously described procedures of the tangent modulus method, the tangent moduli (E_t) of the pile materials at the five instrumentation levels were computed. The results, plotted against the corrected elastic strains, are given in Fig. 9*a*. It can be seen that the tangent moduli at the first two levels sensibly follow a common trend line. This indicates full mobilization of the shaft resistance in the made ground from the early loading stage and that, thereafter, this section of the pile was behaving like a free-standing column. It is important to note that, although the level 1 strain gages were within the steel casing and those at level 2 were not, their resulting modulus values were still very similar. This means that the casing was not contributing to the axial stiffness but was simply floating on the outside of the pile much like a ring on a finger. Although the end effect caused by the closeness of the uppermost gage level to the free end of the pile could have affected the derived E_t values, the remarkable agreement between the measured values at these two levels seems to suggest otherwise. Considering the similar evidence from the previous matching exercise for creep strains, it appears that the casing indeed was not having any measurable impacts on the stiffness of the pile.

The finding of a floating casing is contrary to the common belief that all components contribute fully to the overall pile modulus, so that the transformed area equation can be used to adjust the tangent and (or) secant modulus values (see Table 1). In this case, the steel casing is only one-diameter long, but for piles with longer casings floating may not occur from the very beginning due to the increased contact area. For instance, Finno et al. (2002) showed that in a micropile the strains in the central grout and in the full-length casing remained compatible until about 180 με. Thereafter, the strain in the steel increased at a faster rate than in the grout. They attributed their finding to the debonding between the two materials at their interface.

If one accepts the conclusion about the negligible effect of the steel casing, then the modulus values given in Fig. 9*a* also indicate that the concrete quality was very similar over the top 6.2 m of the pile because of the closeness of the E_t values at gage levels 1 and 2. Because of the size of the pile, the shaft resistance below 6.2 m was not fully mobilized and, hence, the E_t values at gage levels 3–5 did not converge onto the same trend line. This kind of evidence, although somewhat limited in this case, is very important for the strain-to-load conversion process as it is the only piece of evidence that can quantitatively confirm the assumption of uniform concrete quality throughout the pile, which is an assumption used in all of the modulus determination methods. Of course, coring and testing the test pile concrete is another way of validating this assumption, but it is costly and not always possible for small-diameter piles because of verticality or space issues. It is important to note that the assumption of uniform concrete quality should not be confused with the condition of uniform pile geometry, which is another key assumption required by many of the modulus determination methods (see Table 1).

Fig. 9. Tangent modulus plots: (*a*) against elastic strains; (*b*) against total strains.

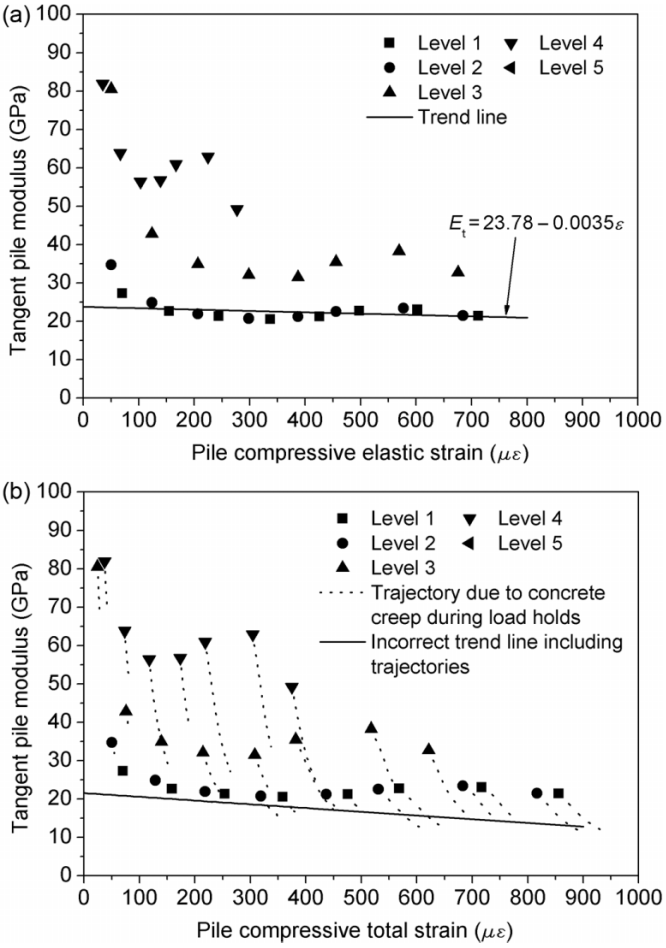

Probably because Fellenius (1980) discouraged the use of "slow" maintained load tests, that is, tests that include load-holding periods such as those specified by ICE (2007) or procedures B and C of ASTM (2007), the tangent modulus method was only demonstrated for "quick" tests in Fellenius (1989, 2001) and the issue of creep strain was not explicitly addressed. As a result, it is not uncommon to see this method also being used for piles showing a noticeable amount of creep (e.g., Holman 2009*b*). To investigate the effect of creep strains on this method, Fig. 9*b* shows the same E_t results as Fig. 9*a* but plotted against the uncorrected total strains. It can be seen that the inclusion of creep strains has two effects: (*i*) it changes the horizontal position of the data points, and (*ii*) it causes the modulus values to drop locally. The first effect is due to the cumulative nature of creep strains on the total measured values, and the second is due to the development of creep strains during the holding periods under constant loads. As can be seen, including the creep strains in the curve-fitting analysis alters the position of the trend line considerably. Tremendous errors can be introduced into the analysis if this is done.

Figure 10 shows the results for the secant modulus method. Both total and elastic strains are again plotted to show the effect of creep on the modulus values. It can be

Fig. 10. Secant modulus plot.

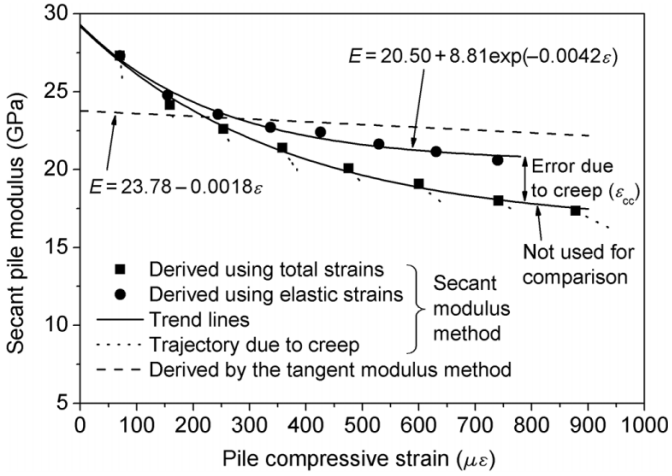

seen that both curves started at the same initial value of about 29 GPa at zero strain. As creep strains started to accumulate during the load test, the curves gradually move apart from each other to as much as 3.5 GPa at 900 με. As was found for the tangent modulus method, if the effect of creep strain is traced throughout the load-holding periods, the data points on the total-strain curve travel downwards as the strains develop, thus introducing errors if these paths are included in the curve-fitting. With regard to the form of the best-fit curve, although in this case an exponential equation has been used to model the change in the modulus value, other forms such as linear, hyperbolic, and polynomial equations have also been used by others (Shi 1996; Omer et al. 2002; Brown et al. 2006; Lee et al. 2006). Also shown in Fig. 10 is the secant modulus line of the tangent modulus method derived using the intercept and the slope of the E_t trend line given in Fig. 9*a*. In terms of the overall value, this line compares reasonably with the secant modulus curve of the secant modulus method, but lacks the flexibility to track the actual response of the pile shown by the solid circles especially at low strains.

Summary of *E* values obtained using different methods

To put the preceding results into perspective, Fig. 11 shows the E profiles of the test pile computed using the six selected methods under the proof load condition (P_h = 18.1 MN). It can be seen that the uncorrected and transformed area methods, both based on the laboratory result of E_c, give significantly higher E values than those based on pile instrumentation. The reasons for this are discussed later. To examine the potential effect of the steel casing, the scenario of full casing effect has been analyzed by the transformed area method. It can be seen that if the casing had bonded perfectly with the concrete and had a full effect on the pile stiffness, it would have locally increased the E of the pile by about 8 GPa. This would have invalidated the assumption of a uniform pile. In this respect, the tangent modulus method is a very useful tool for investigating the response of partially cased piles as any such effects would have shown on the tangent modulus plot. Interestingly, to our knowledge this aspect of the tangent modulus method has not previously been reported. With regard to other instrumentation-based methods, it can be seen that the implicit and

Fig. 11. Summary of derived modulus profiles for the test pile under proof load.

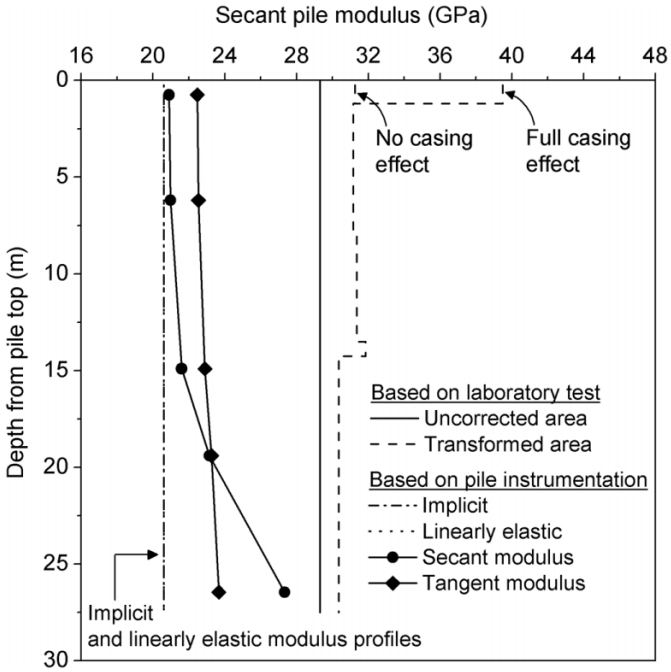

the linearly elastic methods give exactly the same result. Although the linearly elastic method only generates a single value of E for the entire loading range from zero to proof load, and the modulus value effectively used in the implicit method changes only with the applied head load (P_h), under the proof load condition the two values are the same. The two modulus methods, as expected, both give increasing E values with depth due to the reducing level of strain in the pile. The difference in their values is caused by the difference between their parent E–ε relationships as shown in Fig. 10.

Interpreted load distribution

To complete the strain-to-load conversion process, the load distribution along the pile was calculated using eq. [1], the corrected ε profile, and the estimated E profile. Figure 12 shows the results for all six methods. The effect of the residual load on the pile is ignored for the moment but will be considered later. Although in practice the load at the uppermost instrument level is commonly taken as P_h because of the negligible shaft resistance near the surface, it was calculated as a way to assess the performance of the methods. Figure 12 shows many interesting aspects. First, the uncorrected and the transformed area methods grossly overestimate the value of P_h, which is unsurprising as their derived E values are much higher than the others. As the E_c value used by these methods has been checked by considering different evaluation strategies (direct measurement versus correlation from f_{cyl}) and correlation equations (ACI versus Eurocode 2), the problem may therefore lie in the chosen method for obtaining specimens (i.e., casting cubes from the delivery trucks rather than coring the pile). Moreover, the many differences between the laboratory and the field conditions may also contribute to the differences seen. These differences include the scale effect (100 mm versus 1.2 m), different test duration (a few minutes versus a few days), and different

Fig. 12. Summary of interpreted load profiles of the test pile under proof load.

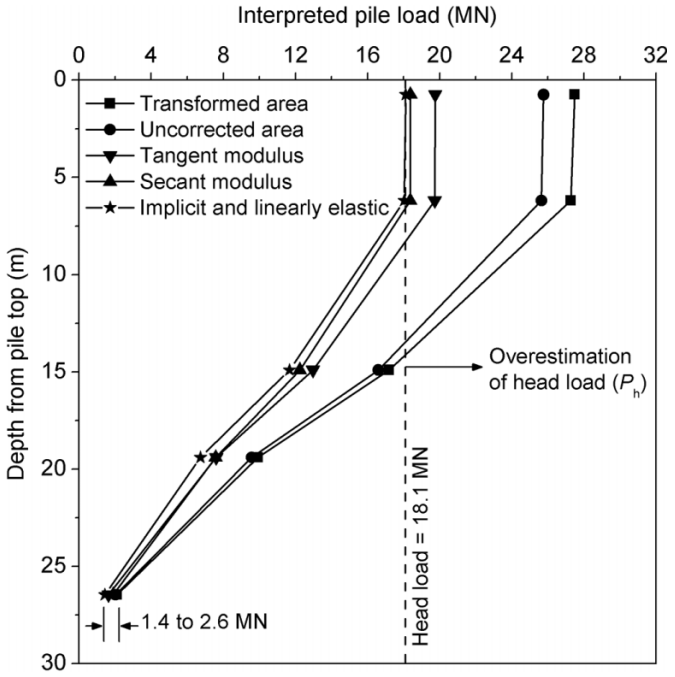

loading rate (0.0006 versus 0.6 ± 0.4 MPa/s). Therefore, however tempting the transformed area method may be (because it is theoretically correct as shown in eq. [2]), it would seem impossible for anyone to estimate E using this method with any degree of confidence unless all of these issues are clearly understood and accounted for.

The results from the two modulus methods are also worthy of discussion. It can be seen that the tangent modulus method overestimates P_h by a small (but noticeable) amount of 1.6 MN (9% of P_h) and the secant modulus method overestimates P_h by 0.3 MN (2% of P_h). This is due to the fact that the E–ε equations used in these methods could differ slightly from the true response by up to a few gigapascal at very high or low strain values. For example, if one accepts the solid circles in Fig. 10 as the "true" stiffness values of the pile, then one can see that under proof load at 739 με the "true" E value is 20.6 GPa, and the tangent and the secant modulus methods give 22.45 and 20.90 GPa, respectively. A similar observation also can be made at small strains such as those smaller than 200 με. Therefore, it would appear that although the assumption of a linear E–ε relation enables the tangent modulus method to include the response of strain gages at more than one level, it also somewhat limits the flexibility of the method as shown in this example.

For the implicit method, the head-load test does not apply, as all the loads are derived as a ratio to P_h; hence the perfect agreement shown in the figure. As mentioned before, as the E value given by the linearly elastic method is numerically the same as that given by the implicit method under proof load, their interpreted load distribution profiles are therefore also the same. However, if a load case other than proof load is analyzed, the linearly elastic method should underestimate P_h as the E value used by this method is a constant while in reality it should rise with increasing depth.

It is also interesting to examine the interpreted loads near the pile toe. Although the difference looks trivial on the plot, there is actually an 86% difference between the lowest and the highest values, which are 1.4 MN given by the implicit and linearly elastic methods and 2.6 MN by the transformed area method. Neither of these values is correct for the various reasons already discussed. The "true" value, however, is believed to be closer to that given by the secant modulus method (1.9 MN) and the tangent modulus method (1.6 MN) as they both allow for the variation of E with depth. However, as will be shown in the following section, this so-called "true" value is not correct either, as it does not take into account the effect of residual load.

Effect of residual load

Regardless of which determination method was used to convert the strain gage results, the shape of the load-distribution curves given in Fig. 12 suggests that the test pile probably had a significant amount of residual load locked-in before the start of the test (see e.g., Fellenius 2002*a* for a discussion of this topic). Although a full analysis of the behavior of the test pile is beyond the scope of this paper, the effect of residual load is considered in this final part to demonstrate its potential effect on the accuracy of the interpreted load. For this particular pile, residual loads could be caused by three mechanisms: (*i*) the recovery of the soil at the pile–soil interface after disturbance caused by the drilling process and the heat and pressure from the fresh concrete; (*ii*) change in concrete volume during curing; and (*iii*) the ongoing consolidation of the clay due to the weight of the recently placed made ground (Fig. 1). In fact, even when the third mechanism does not come into play, some residual loads should still be expected, as was found by O'Riordan (1982) who was working in the nearby area.

To estimate the amount of residual load, the method proposed by Fellenius (2002*b*) was used. In essence, this method assumes that the residual load is fully mobilized along the upper portion of the pile and the soil shearing resistance is independent of the direction of shear. Therefore, the calculated shaft resistance from the measured load curve could be as much as twice the true value for the upper part of the pile. To use this method, one first needs to plot half of the measured load reduction (as calculated from the interpreted strain gage results) against depth and then compare this curve (known as the half curve) with the theoretical shaft resistance obtained from an effective stress analysis. If the assumptions of the method are correct, these two curves should lie on top of each other over the part where the negative skin friction is fully mobilized. The depth where these curves deviate from each other is where the negative skin friction starts to reduce and change to positive direction. Over the "matched length" between these two curves, the residual load is the same as the theoretical shaft resistance (or the values of the half curve), and the true load is therefore the measured load plus the residual load. Because the residual load below the neutral plane cannot be directly determined, it needs to be estimated from the theoretical shaft resistance with the help of some engineering judgment. Further details about this method can be found in Fellenius (2002*b*) and are hence not repeated here.

Figure 13 shows the result of the residual load analysis. The interpreted load curve from the secant modulus method

Fig. 13. True load distribution considering the effect of residual load.

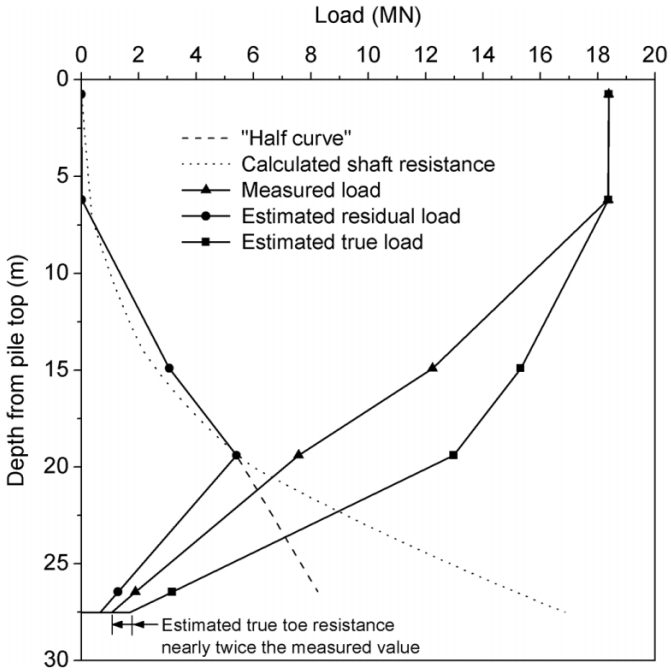

was used as the measured load curve, and the new "half curve" was taken as half of the load reduction from this curve. The theoretical shaft resistance was calculated using the effective stress parameters given in Table 2. As at this stage of the calculation procedure it was not yet known how the pile installation had affected the soil properties at the pile–soil interface, the effective interface angle, δ', was taken as ϕ', and the coefficient of earth pressure for the shaft, K_s, was taken as K_0 (i.e., assuming a wished-in-place pile). It can be seen that the calculated shaft resistance curve lies very close the half curve until a depth of 19 m was reached, which is near the bottom level of the clay layer. The shaft resistance curve was also checked using the total stress approach, and it gave very similar results. To complete the analysis, below the neutral plane both the true and the residual loads were estimated using the calculated shaft resistance curve, and the results are given in Fig. 13. Based on the results of the analysis, it can be concluded that the pile did have a significant amount of residual load locked-in before the start of the test. Ignoring this load would have resulted in significant errors in the interpreted loads. The new load distribution now indicates a toe resistance of nearly twice the originally estimated value.

Conclusions

Despite the importance of the pile modulus to the interpretation of pile load tests, papers on this topic are scattered throughout the literature and there are no definitive recommendations based on critical assessments. Engineers interpreting load tests therefore have to rely on their own experience and may be unaware of the limitations of their chosen method. To improve the situation, this paper first presents the results of a comprehensive survey of the available methods. Ten methods have been identified for the determination of pile modulus, four of which are based on laboratory tests and the remainder on pile instrumentation. The principles and limitations of each method have been discussed.

To assess the performance of the methods, six of them have been used to interpret the results of a slow maintained load test carried out on a bored pile. During the process, special attention has also been paid to the effect of concrete creep strains and the choice of strain-measuring instrument on the derived modulus values. It was found that, even for a pile load test that only lasted for two days, a considerable amount of creep strain developed, which affected the shape of the σ–ε curve and, hence, the derived modulus values. For this test, the sister bar strain gages were found to be more sensitive and reliable than the retrievable-type extensometers, although both instruments have been suggested in the literature. From a comparison of the derived pile modulus and interpreted load distribution profiles, the secant modulus method appears to be the most satisfactory as it is the only method that is free from any obvious problems and yet manages to account for the as-built properties and the strain dependency of the composite pile material. However, its use for interpreting small pile strains (e.g., <80 με) is still subject to uncertainties because of the variabilities in the microstructure of concrete and at the concrete–steel interface. The tangent modulus method, despite its slight overestimation of the head load, has also proven to be a valuable tool in investigating the effect of partial steel encasement and in confirming the quality of the pile concrete with depth. Of course, both these methods require instrumentation on the pile. In contrast, the transformed area method, which is theoretically correct, commonly featured in the literature, and does not require pile instrumentation, grossly overestimates the head load of the test pile, probably due to the chosen sampling method and the difference between laboratory and field conditions. This case study has also shown that, to obtain a representative load distribution, the residual load in the pile should not be ignored; otherwise, considerable errors could result.

Although the case study reported in this paper has served its purpose to demonstrate the strengths and weaknesses of the different modulus estimation methods, the conclusions are confined to this specific case history and pile type. For instance, the transformed area method may perform very differently for other piles, such as continuous-flight-auger and precast driven piles, where the quality of the pile concrete cannot be affected by interaction with the excavation–support fluid. The tangent modulus method also may be the most useful for precast driven piles, as they could have a localized damaged or weakened section due to the impact of driving (Rausche and Webster 2007) and the tangent modulus method is well suited to detect variations in the E value with depth. It would therefore be useful if other researchers who have pile test data could subject them to similar analyses to those presented in this paper and report the findings.

In the section of his book discussing the conversion from strain to stress in concrete, Dunnicliff (1993) says: "stress determination in concrete is by no means straightforward, and accurate results should not be expected". This is a worrying statement, but as shown in this study, Dunnicliff is correct. Stress determination in concrete depends on many factors in-

cluding the assumed model for material behavior and therefore most importantly on the knowledge and experience of the engineers assigned to the task. This study has shown that it is imperative to understand the strengths and limitations of the different methods to make informed decisions on the analysis of pile load tests. The authors hope that the information presented in this paper will make a contribution to the debate of load test assessment.

Acknowledgements

The results presented in this paper were collected as part of a research project funded by an Industrial CASE award by the UK Engineering and Physical Sciences Research Council (EPSRC); grant reference no. EP/C537815/1. Technical support was provided by V. Troughton (formerly Balfour Beatty Ground Engineering), T. Suckling (Balfour Beatty Ground Engineering), C. Martin (Oxford University), A. Blakeborough (Oxford University), P. Martin (Manchester University), M. Pearson (independent), and G. Goodhue (formerly KB International). Additional load test information was provided by A. Proctor and A. Cameron of Environmental Scientifics Group. The comments of K.C. Law and the two anonymous reviewers are gratefully acknowledged.

References

ACI. 2008. Building code requirements for structural concrete and commentary. ACI 318M-08. American Concrete Institute (ACI), Farmington Hills, Mich.

Ali, F.H., Huat, B.B.K., and Lee, S.K. 2008. Pile instrumentation using retrievable sensors. American Journal of Applied Sciences, **5**(5): 597–604. doi:10.3844/ajassp.2008.597.604.

ASTM. 2002. Standard test method for static modulus of elasticity and Poisson's ratio of concrete in compression. ASTM standard C469-02e1. ASTM International, West Conshohocken, Pa.

ASTM. 2007. Standard test method for deep foundations under static axial compressive load. ASTM standard D1143/D1143M-07. ASTM International, West Conshohocken, Pa.

Brown, M.J., Hyde, A.F.L., and Anderson, W.F. 2006. Analysis of a rapid load test on an instrumented bored pile in clay. Géotechnique, **56**(9): 627–638. doi:10.1680/geot.2006.56.9.627.

BSI. 1983. Testing concrete–Part 121: Method for determination of static modulus of elasticity in compression. British standard BS 1881-121:1983. British Standards Institution (BSI), London.

CEN. 2004. Eurocode 2: Design of concrete structures — Part 1-1: General rules and rules for buildings. European standard EN 1992-1-1:2004. European Committee for Standardization (CEN), Brussels, Belgium.

Deschamps, R., and Richards, T.D., Jr. 2005. Installation, measurement and interpretation of "sister bar" strain gauges in micropiles. *In* Proceedings of the GEO Construction QA/QC Technical Conference, Dallas, Tex., 6–9 November 2005. ADSC: The International Association of Foundation Drilling, Irving, Tex. pp. 167–178.

Dunnicliff, J. 1993. Geotechnical instrumentation for monitoring field performance. Wiley InterScience, New York.

England, M., and Fleming, W.G.K. 1994. Review of foundation testing methods and procedures. Proceedings of the Institution of Civil Engineers: Geotechnical Engineering, **107**(3): 135–142.

Fellenius, B.H. 1980. The analysis of results from routine pile load tests. Ground Engineering, **13**(6): 19–31.

Fellenius, B.H. 1989. Tangent modulus of piles determined from strain data. *In* Foundation Engineering: Current Principles and Practices: Proceedings of the 1989 Foundation Engineering Congress, Evanston, Ill., 25–29 June 1989. Geotechnical Special Publication 22. American Society of Civil Engineers, New York. Vol. 1, pp. 500–510.

Fellenius, B.H. 2001. From strain measurements to load in an instrumented pile. Geotechnical News Magazine, **19**(1): 35–38.

Fellenius, B.H. 2002*a*. Determining the resistance distribution in piles. Part 1: Notes on shift of no-load reading and residual load. Geotechnical News Magazine, **20**(2): 35–38.

Fellenius, B.H. 2002*b*. Determining the resistance distribution in piles. Part 2: Method for determining the residual load. Geotechnical News Magazine, **20**(3): 25–29.

Fellenius, B.H. 2009. Citing online sources: views on accuracy of tests and analyses: a slide presentation to the Piling and Deep Foundations Asia Construction Conference, Hong Kong, July 2009 [online]. Available from www.Fellenius.net/papers.html [cited 27 April 2010].

Fellenius, B.H., Kim, S.-R., and Chung, S.-G. 2009. Long-term monitoring of strain in instrumented piles. Journal of Geotechnical and Geoenvironmental Engineering, **135**(11): 1583–1595. doi:10.1061/(ASCE)GT.1943-5606.0000124.

Finno, R.J., Scherer, S.D., Paineau, B., and Roboski, J. 2002. Load transfer characteristics of micropiles in dolomite. *In* Deep Foundations 2002: Proceedings of the International Deep Foundations Congress, Orlando, Fla., 14–16 February 2002. Geotechnical Special Publication 116. American Society of Civil Engineers, Reston, Va. Vol. 2, pp. 1038–1053.

Fleming, W.G.K. 1992. A new method for single pile settlement prediction and analysis. Géotechnique, **42**(3): 411–425. doi:10.1680/geot.1992.42.3.411.

Fleming, K., Weltman, A., Randolph, M., and Elson, K. 2009. Piling engineering. 3rd ed. Taylor & Francis, Abingdon, UK.

GEO. 2006. Foundation design and construction. Geotechnical Engineering Office (GEO) Publication No. 1/2006. Civil Engineering and Development Department, Government of Hong Kong SAR, Hong Kong.

Georgiadis, K., Potts, D.M., and Zdravkovic, L. 2003. The influence of partial saturation on pile behaviour. Géotechnique, **53**(1): 11–25. doi:10.1680/geot.2003.53.1.11.

Gregersen, O.S., Aas, G., and Dibiagio, E. 1973. Load tests on friction piles in loose sand. *In* Proceedings of the 8th International Conference on Soil Mechanics and Foundation Engineering, Moscow, U.S.S.R. Vol. 2.1, pp. 109–117.

Grime, G. 1934. The measurement of impact stresses in concrete. Proceedings of the Physical Society, **46**(2): 196–204. doi:10.1088/0959-5309/46/2/307.

Hanifah, A.A., and Lee, S.K. 2006. Application of global strain extensometer (GLOSTREXT) method for instrumented bored piles in Malaysia. *In* Proceedings of the 10th International Conference on Piling and Deep Foundations, Amsterdam, the Netherlands, 31 May – 2 June 2006. Deep Foundations Institute, Hawthorne, N.J. pp. 669–676.

Hayes, J., and Simmonds, T. 2002. Interpreting strain measurements from load tests in bored piles. *In* Proceedings of the 9th International Conference on Piling and Deep Foundations, Nice, France, 3–5 June 2002. Deep Foundations Institute, Hawthorne, N. J. pp. 663–669.

Hight, D.W., Ellison, R.A., and Page, D.P. 2004. Engineering in the Lambeth Group. Construction Industry Research and Information Association (CIRIA), London. CIRIA Report C583.

Holman, T.P. 2009*a*. High capacity micropiles in Wissahickon Schist bedrock. *In* Proceedings of the International Foundations Congress and Equipment Exposition, Orlando, Fla., 15–19 March 2009. Geotechnical Special Publication 185. American Society of Civil Engineers (ASCE), Reston, Va. pp. 359–366.

Holman, T.P. 2009*b*. Pseudo-elastic response and performance of micropiles. *In* Proceedings of the 9th International Workshop on Micropiles, London, 10–13 May 2009. International Society for Micropiles, Venetia, Pa.

ICE. 2007. ICE Specification for piling and embedded retaining walls. 2nd ed. Institution of Civil Engineers (ICE), London.

Lacy, H.S. 1979. Load testing of instrumented 225-foot-long prestressed concrete piles. Behavior of Deep Foundations. ASTM Special Technical Publication 670. *Edited by* R. Lundgren. American Society for Testing and Materials (ASTM), Philadelphia, Pa. pp. 358–380.

Lee, S.K., Lau, T.K., and Tan, A.H. 2006. Analysis of strain-dependent concrete modulus from mass instrumented test pile samples. *In* Proceedings of the 10th International Conference on Piling and Deep Foundations, Amsterdam, the Netherlands, 31 May – 2 June 2006. Deep Foundations Institute, Hawthorne, N.J. pp. 684–689.

Liew, S.S., Kowng, Y.W., and Gan, S.J. 2004. Interpretations of instrumented bored piles in Kenny Hill Formation. *In* Proceedings of the Malaysian Geotechnical Conference, Petaling Jaya, Malaysia, 16–18 March 2004. Southeast Asian Geotechnical Society, Thailand. pp. 291–298.

O'Neill, M.W., and Reese, L.C. 1999. Drilled shafts: construction procedures and design methods. FHA Publication No. FHWA-IF-99-025. Federal Highway Administration (FHA), U.S. Department of Transportation, Washington, D.C.

O'Riordan, N.J. 1982. The mobilisation of shaft adhesion down a bored, cast-in-situ pile in the Woolwich and Reading beds. Ground Engineering, **15**(3): 17–26.

Omer, J.R., Delpak, R., and Robinson, R.B. 1995. Elastic analysis of a short instrumented composite column for use in the design of large bored piles. *In* Proceedings of the 4th International Conference on Modern Building Materials, Structures and Techniques, Vilnius, Lithuania, 10–13 May 1995. Technika, Vilnius, Lithuania. pp. 230–235.

Omer, J.R., Delpak, R., and Robinson, R.B. 2002. Instrumented load tests in mudstone: pile capacity and settlement prediction. Canadian Geotechnical Journal, **39**(6): 1254–1272. doi:10.1139/t02-072.

Ooi, P.S.K., Lin, X., and Hamada, H.S. 2010. Numerical study of an integral abutment bridge supported on drilled shafts. Journal of Bridge Engineering, **15**(1): 19–31. doi:10.1061/(ASCE)BE.1943-5592.0000037.

Rausche, F., and Webster, S. 2007. Behavior of cylinder piles during pile installation. *In* Contemporary Issues in Deep Foundations: Proceedings of Sessions of Geo-Denver 2007, Denver, Colo., 18–21 February 2007. Geotechnical Special Publication 158. American Society of Civil Engineers (ASCE), Reston, Va.

Sellers, B. 2003. The measurement of stress in concrete. *In* Proceedings of the 6th International Symposium on Field Measurements in Geomechanics, Oslo, Norway, 15–18 September 2003. A.A. Balkema, Rotterdam, the Netherlands. pp. 643–656.

Shi, Y.C. 1996. Critical evaluation and interpretation of instrumented bored cast-in-situ pile load test. *In* Proceedings of the 12th Southeast Asian Geotechnical Conference, Kuala Lumpur, Malaysia, 6–10 May 1996. Southeast Asian Geotechnical Society, Thailand. pp. 385–390.

Stokes, M., and Mullins, G. 2009. Concrete stress determination in rapid load test. *In* Rapid load testing on piles. *Edited by* P. Hölscher and F. van Tol. CRC Press/Balkema, Rotterdam, the Netherlands. pp. 73–100.

Timoshenko, S.P., and Goodier, J.N. 1970. Theory of elasticity. McGraw-Hill, New York.

Wight, J.K., and MacGregor, J.G. 2009. Reinforced concrete: mechanics and design, 5th ed. Pearson Prentice Hall, Upper Saddle River, N.J.

List of symbols

A	cross-sectional area of pile
a	slope of tangent modulus line
b	intercept of tangent modulus line
c	subscript meaning concrete
c'	effective cohesion
cc	subscript meaning concrete creep
E	elastic secant modulus
E_t	elastic tangent modulus
f_{cube}	unconfined compressive cube strength of concrete
f_{cyl}	unconfined compressive cylinder strength of concrete
g	subscript meaning gage
h	subscript meaning pile head
i	subscript meaning the number of instrumentation level, the uppermost level being level 1
K_0	coefficient of earth pressure at rest
K_s	coefficient of earth pressure for the shaft
k	constant of proportionality in design code equations for concrete modulus
L	gage length of retrievable extensometer
P	axial load in pile
RH	relative humidity
S_u	undrained shear strength
s	subscript meaning steel
Z	depth in metres from the top of the relevant soil layer
α	adhesion factor
γ_{sat}	saturated unit weight of soil
δ	pile compression
δ'	effective interface angle
ε	axial strain in pile
σ	axial stress in pile
ϕ'	angle of shearing resistance